Penerbit Akademia Baru

Journal of Advanced Research in
Experimental Fluid Mechanics
and Heat Transfer

Journal homepage:
http://www.akademiabaru.com/submit/index.php/arefmht
ISSN: 2756-8202

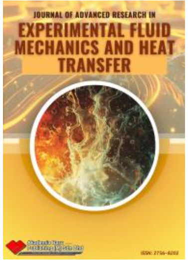

Lithium Bromide-Water Absorption Refrigeration System Driven by Automobile Exhaust Gas: Thermodynamic Study

Mohammed Qasim Alomary[1,*], Salman Hashim Hammadi[1]

[1] Department of Mechanical Engineering, College of Engineering, University of Basrah, Basrah, Iraq

ARTICLE INFO

Article history:
Received 18 March 2025
Received in revised form 10 April 2025
Accepted 9 May 2025
Available online 30 June 2025

ABSTRACT

This manuscript conducts a thermodynamic investigation into the feasibility of using engine waste heat as exhaust gas to operate a 5 Kw cooling capacity of a lithium bromide-water Absorption Cooling System (ACS). We investigated the Performance Coefficients (COP) of the generator, condenser, absorbent and evaporator at different temperatures, as well as the impact of the heat exchanger effectiveness on the system COP. The results indicate that the system performance was more effective at high evaporator and generator temperatures; at generator temperature 90 °C and evaporator temperature 5 and 15 °C, it was 0.7398 and 0.8228, respectively and low absorber and condenser temperatures. The COP was 0.7617 at the condenser and generator temperatures of 40 and 90 °C, respectively. At the same conditions, the COP was 0.8082 at the condenser temperature of 30 °C. Additionally, the increased effectiveness of the solution heat exchanger leads to an increase in the COP. At the condenser, evaporator, generator, absorber and effectiveness (40, 7, 90, 35 °C and 0.6), the COP was 0.7781. At the same temperature and 0.9 effectiveness heat exchanger, COP was 0.8321, while the circulation ratio remained unchanged.

Keywords:
Lithium bromide; waste heat; exhaust gas; absorption cooling system

1. Introduction

Modern progress is primarily driven by the necessity for a diverse array of energy sources. In response to the growing energy demand, there is a need to identify new energy sources or innovative processes that can increase energy efficiency. Most thermal engines are based on fossil fuels and internal combustion engines (ICE) are among the most widely used and mature [1,2]. One of the obstacles faced by these engines is the need to decrease their greenhouse gas emissions and enhance their efficacy [3]. In fact, the ICE converts only one-third of the energy it receives into mechanical work [4-6]. The exhaust and cooling systems are responsible for losing the remaining energy. The most often used cooling technique in automobiles nowadays is the vapour compression cycle (VCS). However, the refrigerants used in VCS are primarily hydrocarbons, such as HCFCs and HFCs, which are not environmentally friendly. This leads to undesirable changes to the environment and

---

[*] *Corresponding author.*
E-mail address: engpg.mohammed.qasim@uobasrah.edu.iq (Mohammed Qasim Alomary)

https://doi.org/10.37934/arefmht.20.1.102120

atmosphere, such as global warming and the depletion of the ozone layer. Furthermore, the system places additional demands on the system to ensure that the engine shaft's power is sufficient to operate the vapor compression system's condenser. This leads to the accumulation of excessive energy and work, which in turn leads to negative environmental changes. One of those solutions is the absorption cooling system, which operates on a heat source. Consequently, the exhaust can transfer the residual heat from the engine to the system, thereby reducing fuel drainage and emissions [7-11].

Detailed reviews use of exhaust gas produced during engine combustion and some other sources to power the ACS can be seen in review papers by several authors [12-27].

Koehler *et al.,* [12] tested and improved the exhaust gas-heated Absorption Refrigeration System (ARS) prototype using a 420-horsepower diesel engine. Insufficient exhaust emissions powered a 4-kW absorption system for 20%, 40% and 80% of its operation. Lin *et al.,* [13] revealed that diesel engine exhaust waste heat was insufficient to run a commercial Diffusion Absorption Refrigerator (DAR) when engine capacity exceeded 50%. COP was 0.034, which is poor. Not for use in an automotive, the configuration tested DAR functioning and engine exhaust connection. Manzela *et al.,* [14]. An internal combustion engine-powered ammonia-water DAR exhaust was examined. After three hours, the refrigerator maintained a temperature of 4-13 ℃, depending on engine throttle valve opening. Anurodh Mohapatra *et al.,* [15] A 10.55-kilowatt absorption chiller might use a 2.8-liter V6 diesel engine. They stated that the system's dependability, ammonia or lithium bromide regulatory problems and cost-benefit analysis of the extra weight need further examination. Automobile ARS may also use engine exhaust. Rêgo *et al.,* [16] conducted ammonia-water absorption cooling experiments. The microcontroller controls exhaust gas. Exhaust heat powered the absorption system between 1500 and 4300 rpm, except at 1000. Evaporation temperature dropped more between 1500 and 2500 rpm than at higher engine speeds. The generator's wide temperature range allowed the system to drop to a little over 0 °c [17]. A LiBr-H_2O of ARS powered by engine exhaust was built. With a 1.3 L engine, the system achieved a cooling capacity of 2.5 kW. The ARS performance was directly influenced by engine performance. At an evaporator temperature of 11°C, the COP recorded was 0.78. The ARS demonstrated optimal performance when the recovered exhaust heat was less than 9 kW. Aly *et al.,* [18] assessed the thermal performance of a DAR system powered by the heat from diesel engine exhaust. Experiments indicated that the DAR system could manage exhaust emissions across engine capacities. The refrigerated cabin reached 10–14.5°C at 3.5 hours after system activation, depending on engine load [19]. DAR system experiments used engine exhaust gas and grid energy for heat exchange. Thermodynamic balances and heat transfer studies explained component behaviour. Exhaust and electrical sources ran at 140°C–152°C. They found exhaust gases can power DAR. H. Yuan *et al.,* [20] proposed an ARS marine engine exhaust gas heat recovery experiment. They employed NH_3–H_2O–LiBr for this system. In experimental operation, a prototype absorption device reduced rectifier heat exchange area by 16%. The ternary system runs below -15.0°C, unlike the binary system [21]. The single-effect LiBr-H_2O-based ARS was tested with 4-stroke gasoline engine exhaust. The ARS works best with an engine between 1200 and 1400 (rpm), according to experiments at 1000, 1200, 1400 and 1600. Higher effluent temperatures enhance generator temperatures, promoting LiBr-H_2O solution crystallization at rates over 1600 rpm. COP was 0.275 at 1400 rpm with a 700 W cooling load.

Kaynakli *et al.,* [22] investigated lithium bromide and water thermodynamics. When absorber and condenser temperatures drop, evaporator and generator temperatures rise (COPc) and COP. Thus, the solution heat exchanger (SHE) affected parameters more than the refrigerant heat exchanger. The SHE increases COP by 44%, while the RHE increases it by 2.8%. Sharma *et al.,* [23] used a hot water-driven, single-stage LiBr-H_2O ARS to study how different variables affect COP. The graph illustrates condenser pressure rising with evaporator pressure. COP falls as condenser pressure rises. The absorber's LiBr solution concentration decreases, increasing the COP [24]. With a 195-kW marine engine, the suggested onboard absorption device will be tested. A typical Italian fishing vessel cooling load can save fuel consumption by 1,600 kg and CO_2 emissions by three tones. Fuel savings are seven times greater for larger vessels with 10 kW cooling. Zheng *et al.,* [25] studied the "Solar-Assisted Absorption Refrigeration System" (SAARS) thermodynamically. The solar collector, generator, condenser and evaporator were examined for entropy generation and irreversible losses. The COP was 0.747 and the total entropy generation was 16–27 W/K. At 75.83%, the solar collector caused the most permanent losses. Kumar *et al.,* [26] designed a SAARS for an office building with an area of 100 m^2. A genetic algorithm was used to optimize the system's operating parameters in order to maximize the COP. The ideal solar collector area was determined to be 14.6 m^2 and the system can operate year-round because the storage volume needed to satisfy the cooling load is 0.48 m^3, taking into account changes in solar radiation and ambient temperature. %. Ammar *et al.,* [27] studied analysis of the ARS employing jacket cooling solutions and shipboard diesel engine exhaust gasses. Its solvents were LiBr-H_2O. VARS reduced annual fuel usage by 156 tons and pollutants by 6.3% compared to the main engine during a cruise.

This manuscript conducts a thermodynamic investigation into the possibility of using engine waste heat as exhaust gas to operate a 5 Kw cooling capacity of the LiBr-H2O absorption cooling system. We studied the performance coefficient at different temperatures of the generator, condenser, absorbent and evaporator, as well as the impact of the heat exchanger's effectiveness and the strong/weak solution concentration on the system performance coefficient. Although, the effect of these operational parameters on COP has not been sufficiently analysed in previous studies in terms with automotive applications. This gap is sought to be filled with the development of a mathematical model to optimize system performance.

1.1 Automobile Engine Balance

The energy included in petroleum is, however, only a small amount of it is converted to power output, despite the substantial technological advancements made by modern automotive engines. Still, the maximum efficiency is less than 40%. Exhaust gases and coolants are responsible for most losses, which are emitted into the environment as heat. An automotive engine energy balance shows how the fuel's energy is used and wasted. Nevertheless, only a small portion of the energy generated is needed for the mechanical work. As he remains inside the cylinder, the leftover energy is actually released in a few other locations. A first-law analysis yield for a car engine.

$$\dot{Q}_{in} = W + \dot{Q}_{co} + \dot{Q}_{ex} + \dot{Q}_r \qquad (1)$$

where, $\dot{Q}_{in}$ "is the heat supplied to the engine", $\dot{Q}_{co}$ heat that is transmitted to the cooling system, $\dot{Q}_{ex}$ exhaust gas heat rejection, $\dot{Q}_r$ the amount of heat unconfined into the environment, W the output of mechanical energy. The energy balance of a contemporary automobile engine is illustrated in Figure 1. The heat that is transferred to coolants (25-30%) and the heat that is denied in the exhaust gas (30%) and (35%) for power; finally, radiation releases a minuscule portion of the energy (5%). At first glimpse, the heat flow analysis indicates that there are two engine waste heat streams with the potential to be recovered, each at a distinct temperature: exhaust gas (250-600°C) and cooling water (75-100°C).

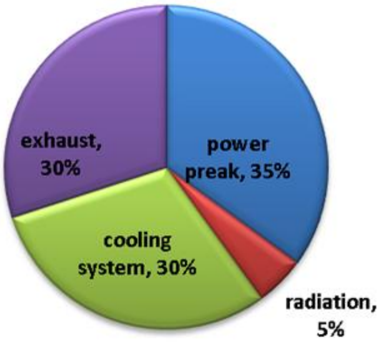

Fig. 1. Total percentage of waste energy in engine

2. Methodology

This section details the methodology required for constructing and analysing an ACS which uses car exhaust gas as its power source. The proposed system utilizes waste heat from exhaust gases to operate its cooling cycle which improves system efficiency while minimizing environmental impact.

2.1 System Description

The ACS incorporates seven primary components, as illustrated in Figure 2: a generator, condenser, evaporator, absorber, compressor and heat exchanger. Specifically, the cycle includes two expansion valves. The two primary fluids circulate throughout the system are refrigerant and absorber. The low-pressure absorber (state 1) transfers a weak absorbent/refrigerant through a pump (state 2) and solution heat exchanger (state 3) to the tall-pressure generator [28]. High-pressure vapor is subsequently condensed to a saturated liquid (state 7) within the condenser. Following the passage of the saturated high-pressure liquid through an expansion valve (state 8), its temperature decreases due to the liquid's reduced pressure. Saturated low-pressure liquid refrigerant is converted to low-pressure vapor in the evaporator (state 9). The absorbent subsequently absorbs the vapor as it enters the absorber (state 10). After separating from the refrigerant, the generator residual strong absorber will be returned to the absorber. At a high temperature (state 4), the weak solution travels in the opposite direction from the absorber to the generator and exchanges heat with the strong solution. Afterward, the expansion valve (state 5) reduces the strong absorber pressure to the absorber pressure level. A chemical compressor is a collective term used to describe the absorber, pump, generator and expansion valve cycle [29].

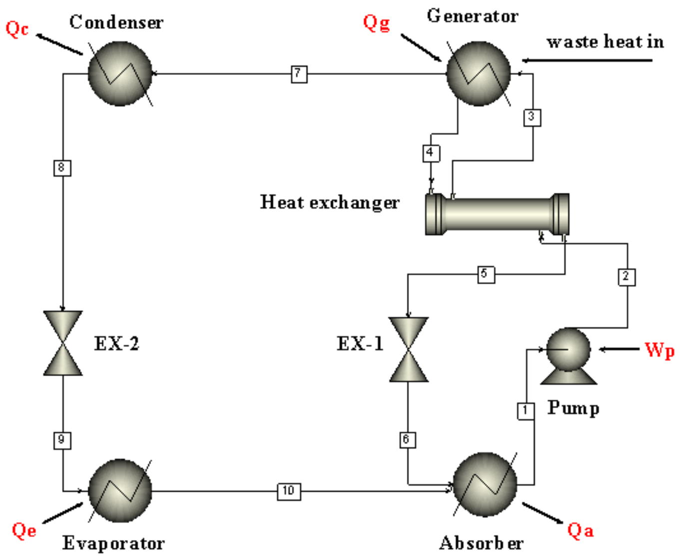

Fig. 2. Schematic of ACS powered by exhaust gas engines

2.2 Model Setup

This manuscript uses MATLAB owing to its straightforward technical language. MATLAB allows the building of mathematical models for absorption cooling systems, especially in the thermal liquid domain, where internal and external processes modify temperature and viscosity. Table 1 displays the simulation input settings and limitation data. Calculate enthalpy, mass flow rate, refrigerant concentration, pressure and COP using these parameters.

2.3 Thermal Analysis

To perform a thermodynamic analysis, we subjected each system component inflow and exit streams, as well as the exchange of heat and work with the environment through each control volume, to mass and energy conservation laws. Table 1 displays the simulation input settings and limitation data.

Table 1
Fixed simulation data

Generator temperature (°C)	75-90
Condenser temperature (°C)	30-40
Evaporator temperature (°C)	5-15
Absorber temperature (°C)	25-35
Solution heat exchanger effectiveness	0.5-0.9
The evaporator (cooling capacity, Kw)	5

We have simplified the theoretical model by incorporating the following assumptions [25,30]:

i. All points of the cycle are assumed to be in thermodynamic equilibrium and the analysis is conducted under “steady-state conditions”.
ii. Refrigerant and solution expansion valves operate adiabatically.
iii. Every component and the connecting pipelines demonstrate negligible heat transfer and pressure loss to the environment.

iv. The condenser, evaporator, generator and absorber temperature fluctuations are negligible.
v. The pressure in the evaporator-absorber and generator-condenser pairs is comparable.
vi. Eq. (8) outflow of the condenser and Eq. (10) outlet of the evaporator, the refrigerant is saturated liquid and saturated vapor, respectively.
vii. The server's refrigeration circuit facilitates heat transfer to the evaporator.

2.3.1 Mass and energy at every element

The governing equations for the conservation of mass and energy must be applied to each component and the entire system in order to develop our thermodynamic model for this system. The equations in consideration employ the following general forms:

$$\frac{dm}{dt} = \sum_{in} \dot{m} - \sum_{out} \dot{m} \tag{2}$$

$$\frac{dE}{dt} = \dot{Q} - \dot{W} + \sum_{in} \dot{mh} - \sum_{out} \dot{mh} \tag{3}$$

The empirical equation developed by is employed to ascertain the associated pressures when the condenser and evaporator temperatures are known [11]:

$$p = \exp\ (9.48654 + \frac{3892.7}{42.6776-T}) \tag{4}$$

Equations presented are employed to determine the concentration of LiBr in the strong and weak solutions (X_{ss}) and (X_{ws}) respectively:

$$X_1 = X_{ws} = \frac{49.04+1.125T_a-T_e}{134.65+0.47T_a} \tag{5}$$

$$X_5 = X_{ss} = \frac{49.04+1.125T_g-T_c}{134.65+0.47T_g} \tag{6}$$

The mass and energy balance of evaporator (Q_e) is given by:

$$Q_e = \dot{m}_{10}h_{10} - \dot{m}_9h_9 \tag{7}$$

$$Q_e = \dot{m}\ (h_{10} - h_9) \tag{8}$$

(h_9, h_{10}) Enthalpy of saturated liquid and saturated vapour refrigerant (kJ/kg), we can calculate by the following equation:

$$h_{10} = 2501 + (1.88 * T_e) \tag{9}$$

$$h_9 = 4.19 * T_c \tag{10}$$

The mass and energy balance of condenser (Q_c) we can calculate as follows:

$$Q_c = \dot{m}\ (h_7 - h_8) \tag{11}$$

The energy balance of heat exchanger:

$$Q_{HE} = \dot{m}_{ws}(h_3 - h_2) = \dot{m}_{ss}(h_5 - h_4) \tag{12}$$

$$\varepsilon = \frac{(T_g - T_5)}{(T_g - T_a)} \tag{13}$$

By using Eq. (13) we can calculate the temperature outlet of heat exchanger solution (T_5). The following relationship can be employed to ascertain the specific heat of a weak solution [11]:

$$C_{ws} = 4.184 * (1.01 - 1.23\, X_{ws} + 0.48\, X_{ws}^2) \tag{14}$$

The following relationship can be employed to ascertain the specific heat of a strong solution:

$$C_{ss} = 4.184 * (1.01 - 1.23\, X_{ss} + 0.48\, X_{ss}^2) \tag{15}$$

The temperature at which the solution exits the heat exchanger:

$$T_3 = T_a + [\varepsilon * \left(\frac{X_{ws}}{X_{ss}}\right) * \left(\frac{C_{ss}}{C_{ws}}\right) * \left(T_g - T_a\right)] \tag{16}$$

Enthalpy of solution at (state 1) and (state 5) outlets can be calculated from solution temperature and concentration using standard formulae provided by Kaita [30]:

$$h(T, X) = (A_0 + A_1 X)T + 0.5(B_0 + B_1 X)T^2 + (D_0 + D_1 X + D_2 X^2 + D_3 X^3) \tag{17}$$

where, (20 ≤ T ≤ 210 °C), absorbent concentration (40 ≤ X ≤ 65 wt.%):

$$\begin{array}{lll} A_0 = 3.462023 & B_0 = 1.3499e^{-3} & D_0 = 162.81 \\ A_1 = -2.679895e^{-2} & B_1 = -6.55e^{-6} & D_1 = -6.0418 \\ & & D_2 = 4.53488e^{-3} \\ & & D_3 = 1.2053e^{-3} \end{array}$$

Now we can calculate the enthalpy of point (7,1) by using the above equation and substance in Eq. (17) to calculate (Q_a). Absorber is given by the following equations:

$$Q_a = \dot{m}_{10}h_{10} + \dot{m}_6 h_6 - \dot{m}_1 h_1 \tag{18}$$

Circulation ratio (λ) is computed using the following formula [28]:

$$\lambda = \frac{\dot{m}_{ss}}{\dot{m}} \tag{19}$$

$$\lambda = \frac{X_{ws}}{X_{ss} - X_{ws}} \tag{20}$$

The value of the rate of heat addition in the generator (Q_g) is as follows:

$$Q_g = \dot{m}_7 h_7 + \dot{m}_4 h_4 - \dot{m}_3 h_3 \tag{21}$$

Determine the strong solution density at state of Eq. (1) to ascertain the pump work. The equation is employed to acquire it [31]:

$$\rho = 1145.36 + 470.84X_{ws} + 1374.79X_{ws}^2 - (0.333393 + 0.571749X_{ws})T \tag{22}$$

The work done by the pump is [9]:

$$W_p = \frac{\dot{m}_{ws}(p_c - p_a)}{\rho} \tag{23}$$

2.3.2 The performance of ACS

The COP is typically employed to evaluate the performance of refrigeration systems. As the energy input of the system is divided by the useful effect produced, this parameter is defined as:

$$cop = \frac{Q_e}{Q_g + W_p} \tag{24}$$

2.4 Available Heat in the Exhaust Gas

In our system, the ACS will act as a heat exchanger, with the heated exhaust gas from the engine passing through the generator, which functions as a vapor absorption generator. The heated exhaust gas is heat-absorbed by the cold fluid, an H2O-LiBr solution, as it passes through the generator.

Table 2
Performance data for a 180 HP engine in tabular form

Speed rpm	Engine load (Torque) NM	Exhaust Mass flow rate Kg/s	Exhaust temperature k
1000	581	0.038	585
1100	586	0.043	579
1200	658	0.051	593
1300	660	0.059	593
1400	662	0.065	581
1500	653	0.075	579

The inlet temperature of the hot exhaust gas is T_h = 585 K and the mass flow rate of the exhaust hot gas was 0.038 at 1000 rpm.

The exhaust gas maximum thermal capacity:

$$Q_h = C_h \Delta T \tag{25}$$
$$Q_h = 0.038 * 1.1 * (585 - 285) = 12.54\ kw$$

The previously indicated result indicates that the vehicle's engine exhaust has sufficient energy to run the ACS. This heat was transferred to the system solution by the generator, which usually consists of a shell and a tube.

3. Result and Discussion

MATLAB program was used to estimate the properties and energy of the LiBr absorption cooling system, ensuring the accuracy of the generated thermodynamic model. To verify the present model, we compared the output results of the energy calculation with those of Rubio-Maya *et al.,* [32]. The discrepancy between our model's results and the individuals of Rubio-Maya *et al.,* [32] was less than 3.3%. The model's discrepancies in the calculation of refrigerant properties, specific heat solution and density are the most probable causes of the deviations. Additionally, the proposed model results have been compared with the experimental results of Patel *et al.,* [33] to validate the present model. The differences in COP value were 8.23 %. The comparison study has been listed in Table 3 and Table 4. The programs use subroutines to calculate the binary solution's thermodynamic characteristics in response to temperature and concentration [30].

Table 3
Validation of the present study with Rubio-Maya *et al.,* [32]

Variable/parameter	Data type	Symbol (unit)	Data of Rubio-Maya *et al.,* [32]	MATLAB Model-present study	Deviation %
Generator temperature	input	$T_g(^\circ C)$	84.8	84.8	-
Condenser temperature	Input	$T_c(^\circ C)$	39.8	39.8	-
Evaporator temperature	Input	$T_e(^\circ C)$	8.6	8.6	-
Absorber temperature	Input	$T_a(^\circ C)$	35.5	35.5	-
The effectiveness of heat exchanger	input	ε	0.707	0.707	-
Evaporation heating load	input	$Q_e(kw)$	201.29	201.29	-
Generator heating load	Output	$Q_g(kw)$	259.55	251.56	3
Condenser heating load	Output	$Q_c(kw)$	213.37	206.31	3.3
Absorber heating load	Output	$Q_a(kw)$	247.47	246.18	0.5
Coefficient of performance	Output	COP	0.7755	0.8001	3.07

Table 4
Comparison of the proposed model with the experimental results of Patel *et al.,* [33]

Perimeters: $\boldsymbol{T_g = 80}$ °C, $\boldsymbol{T_e = 13}$ °C, $\boldsymbol{T_a = T_c = 40}$ °C, effectiveness of heat exchanger =0.5			
Component	Patel *et al.,* [33] (Model result)	Present study	Discrepancy (%)
	Q(KW)		
Generator	200.8	185.642	9.17
Condenser	158.56	143.013	9.8
Absorber	195.84	182.388	6.68
Evaporator	140	140	-
COP	0.692	0.7541	8.23

Table 5 shows a quantitative comparison of our work with Ammar *et al.,* [27]. Our investigation increased the performance coefficient by 1.13 %, although the results were mostly similar to Ammar's.

Table 5
Quantitative comparison of the proposed model with the Ammar *et al.,* [27]

Perimeters: $\boldsymbol{T_g = 90}$ ℃, $\boldsymbol{T_e = 6.7}$ ℃, $\boldsymbol{T_a = T_c = 30}$ ℃, effectiveness of heat exchanger =0.7

Component	Ammar *et al.,* [27]	Present study	Discrepancy (%)
	Q(KW)		
Generator	312	298.894	4.2
Condenser	256	254.586	0.55
Absorber	298	293.901	1.37
Evaporator	250	250	-
COP	0.827	0.8364	1.13

The system circulation ratio and COP are influenced by the combined temperatures of the generator and condenser, as demonstrated in Figure 3. The temperatures of the evaporator and absorber are maintained at 7°C and 35°C, respectively. The heat exchanger solution effectiveness was identified to be 0.5. The COP generally increases as the generator temperature increases, as illustrated in Figure 3(a). Furthermore, the COP decreases as a result of the elevated condenser temperature. It is important to note that the system cannot be accomplished for each condensation temperature, the generator temperature is below the lower limit. For example, when the condenser temperature was (30-35-40 °C), the acceptable COP was (0.8082, 0.7887, 0.7617) and the temperatures T_g correspond to the acceptable COP (90 °C). When generator temperatures go close to their lower bounds, the circulation ratio rises significantly Figure 3(b). Increased circulation ratio values necessitate unsuitable solution pump size. This clarifies why a cycle cannot be completed at extremely low generator temperatures. The circulation ratio rises as the condenser temperature rises.

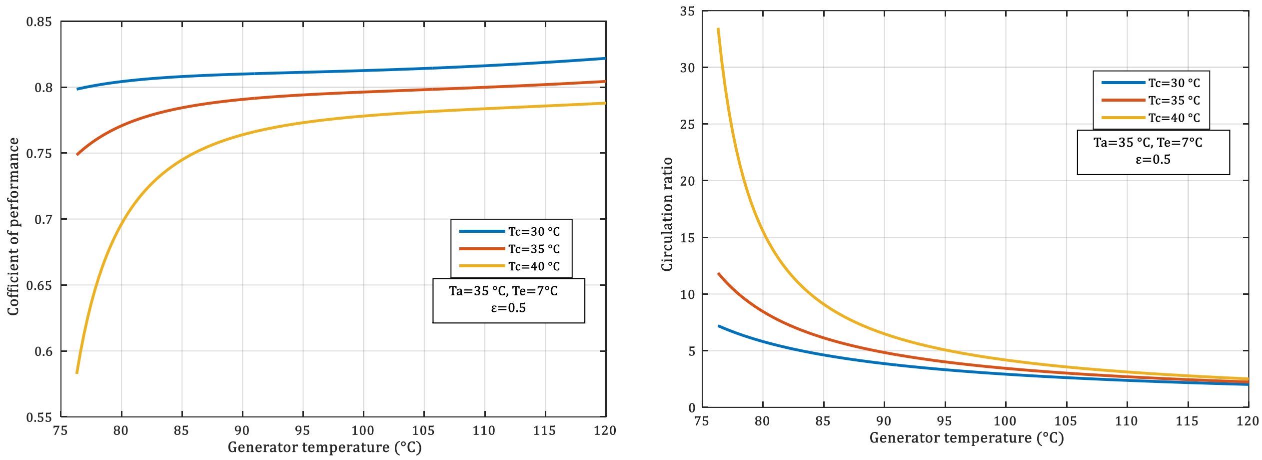

(a) (b)

Fig. 3. The influence of generator temperatures at different condenser temperatures on (a) COP (b) Circulation ratio

The interplay between the temperatures of the absorber and generator has a similar impact on the circulation ratio and COP as shown in Figure 4, which is comparable to the effects of the condenser temperature. As the "absorber temperature rises, the circulation ratio also increases", but the maximum COP value of the system drops, as illustrated in Figure 4(a). The reason for this is that when the absorber temperature is increased, the proportion of H_2O in the weak solution decreases, while the proportion of other components remains unchanged. The generator emits a reduced amount of H_2O into the refrigeration cycle, leading to a decreased COP. In addition, the circulation ratio increases due to the decrease in the disparity of the solution mass fraction between the weak and strong solutions in the generator. At a generating temperature of 90 °C, the maximum COP values is 0.8041, 0.7857 and 0.7617, respectively.

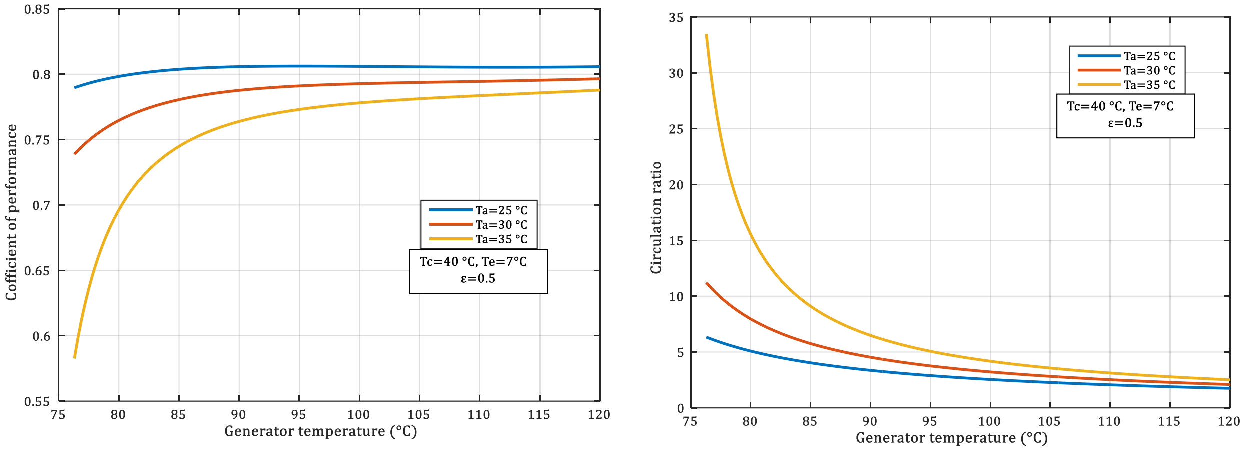

(a) (b)

Fig. 4. The influence of generator temperatures at different absorber temperature on (a) COP (b) "Circulation ratio"

The combined impact of the evaporator and generator temperatures is demonstrated in Figure 5, which also displays the circulation ratio and COP. Heat exchanger solution effectiveness was determined to be 0.5 at evaporation temperatures of 5, 10 and 15°C, with the absorber and condenser temperatures fixed at 35°C and 40°C, respectively. As the temperature of the generator increases, the COP increases abruptly until it reaches its optimum. The cooling output energy of the system is increased as a result of the separation of more refrigerant from the mixture and its subsequent entry into the refrigeration cycle as the generator temperature increases. However, the mass fraction of H_2O in strong solution (state 4) decreases, requiring a greater amount of energy to separate. In the same condition as the evaporator increases, the COP of the system increases and the maximal value of COP also increases, as illustrated in Figure 5(a). For example, the COP is 0.7398 at 5 °C, 0.7881 at 10 °C and 0.8228 at 15 °C when T_g is 90 °C. The highest COP values are 0.8228 at 15 °C. The mass fraction of water in the X_{ws} (state 1) rises because the pressure of both the evaporator and the absorber increases as T_e increases. As a result, the refrigeration cycle contains an increased quantity of refrigerant that is separated. The generator's system operates more efficiently.

Figure 5(b) demonstrates similar rises in the circulation ratio when generator temperatures approach their minimum values. Then, at generator temperatures below 100°C, the evaporation temperature drops, increasing the circulation ratio. After this point, the circulation ratio is not significantly affected by the generator and evaporator temperatures.

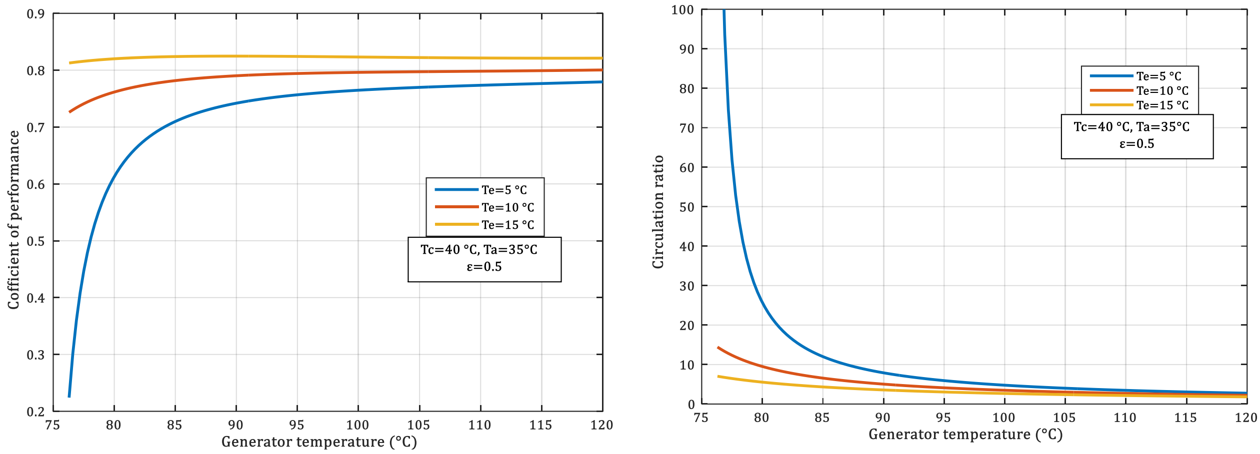

(a) (b)

Fig. 5. The influence of generator temperatures at different evaporator temperatures on (a) COP (b) "Circulation ratio"

With the generator, evaporator, condenser and multi absorber temperatures set to 90, 7, 40 and (30, 35, 40°C) respectively. Figure 6 shows the system performance and circulation ratio at various solution heat exchanger effectiveness. As illustrated in Figure 6(a), the COP is considerably increased by an increase in effectiveness. On the other hand, it does not affect the circulation ratio of the cycle, as showed in Figure 6(b).

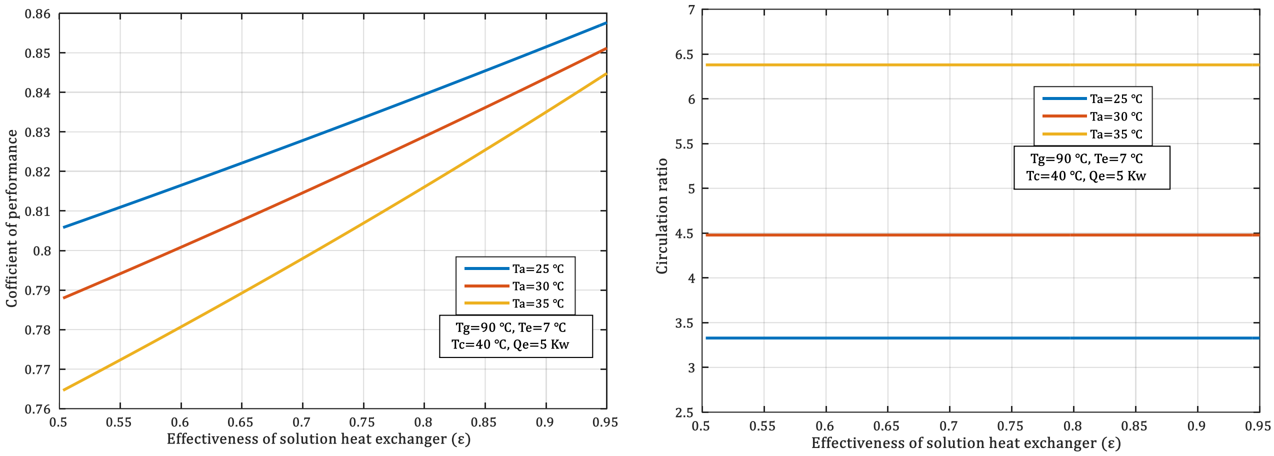

(a) (b)

Fig. 6. Effect of effectiveness heat exchanger at varied value of absorber temperature on (a) COP (b) circulation ratio

An investigation also shows that the COP drops as the X_{ws} in a LiBr-H_2O absorption The refrigeration system expands, as illustrated in Figure 7(a). This is because the heat absorption by the absorber reduces, energy input in the generator is more, pressure is raised and more energy is required to handle. Finally, all these changes lead to reduced system efficiency and increased operational expenses.

When the X_{ss} going backward through the generator and the absorber is high, the concentration difference between the strong solution and water vapor going into the absorber is large. This difference increases the possibility of the strong solution to pick up water vapor more in the absorber. At low absorber temperatures, the utilization of the strong solution is high since the absorption reaction of lithium bromide and water is more favoured at lower temperatures. When the concentration was 0.55 and 0.6, the COP was 0.75 and 0.8, respectively, at an absorber temperature of 30°C observed as Figure 7(b). These values were obtained under the same conditions as:

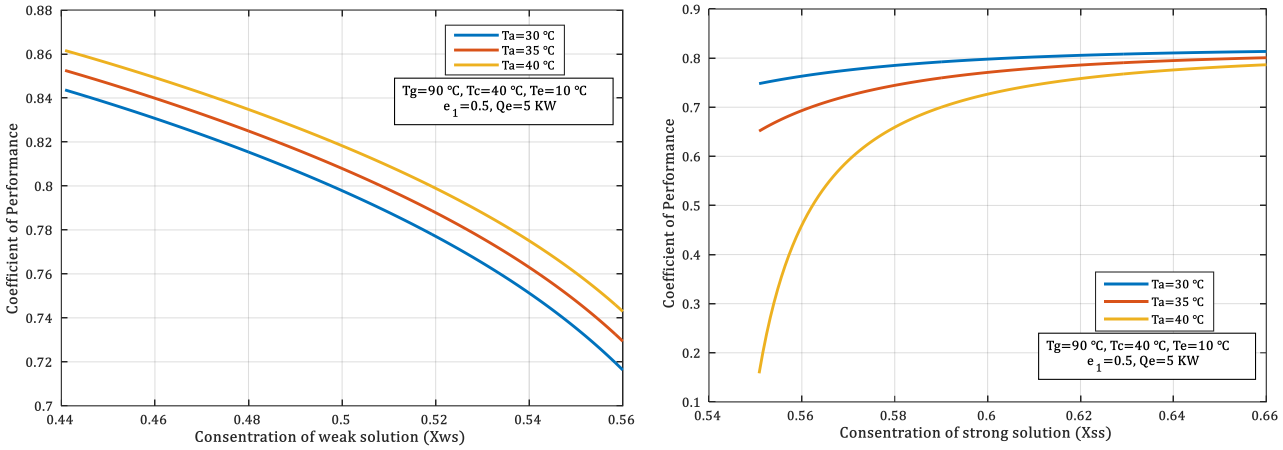

(a) (b)

Fig. 7. Influence of concentration on COP (a) weak solution (b) strong solution

When the refrigerant flow rate is high especially in the Lithium Bromide-Water system, then a greater mass flow rate of the refrigerant gets to the evaporator as illustrated on Figure 8. This leads to attainment of greater heat transfer of the cooled medium to the refrigerating system, thereby improving the cooling capacity. High flow rates improve heat transfer between the refrigerant and the medium of the evaporator. That is because flat plates finned can dissipate heat more effectively than the cooled medium it constantly circulates.

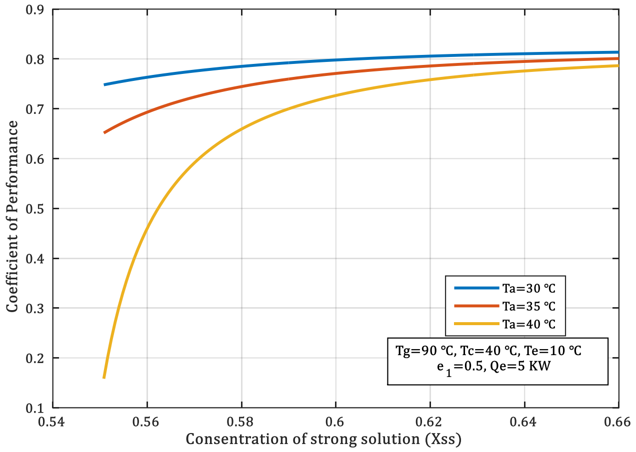

Fig. 8. Influence of refrigerant mass flow rate on cooling capacity

The thermodynamic properties of the system are summarized in Table 6 and Table 7. The temperatures of the generator, condenser, absorber and evaporator were 90, 40, 35 and 7 °C, respectively. Table 7 displays the coefficient performance of the system and the heat transfer for each component. Additionally, Table 6 displays the temperature, pressure, specific enthalpy, LiBr mass concentration and mass flow rate for each point in the system, as indicated by the numbering in Figure 2.

Table 6
Thermodynamic properties of ACS

Point	$h(\frac{kj}{kg})$	$T(°C)$	$P(kpa)$	$m(\frac{kg}{s})$	X
1	79.677	35	0.990	0.01269	0.538
2	79.677	35	7.359	0.01269	0.538
3	123.741	54.65	7.359	0.01269	0.538
4	222.243	90	7.359	0.01057	0.623
5	170.970	62.5	7.359	0.01057	0.623
6	170.970	62.5	0.990	0.01057	0.623
7	2576.2	90	7.359	0.00212	0
8	167.600	40	0.990	0.00212	0
9	167.600	40	0.990	0.00212	0
10	2514.2	7	0.990	0.00212	0

Table 7
Heat transfer in each component and COP of ACS

The system component	Q (W)
Q_e	5000
Q_g	6344.3
Q_c	5119.9
Q_a	6218.2
Q_{HE}	536
COP	0.7617

3.1 Performance Parameter Evaluation

A comparative analysis was carried out to assess the effect of various operational factors on the performance of the absorption cooling system using lithium-water bromide solution. This analysis aims to understand how generator, condenser, evaporator and absorbent temperatures, as well as the effectiveness of heat exchangers and weak solution concentration, affect system efficiency and COP. The results are shown in the Table 8, where each variable is analysed with the other values fixed to ensure the accuracy of the evaluation.

3.1.1 Effect of generator temperature (T_g)

As shown in Table 8, an increase in the temperature of the generator leads to a slight improvement in the COP, rising from 0.7634 at T_g = 80°C to 0.7983 at T_g= 110°C. This improvement is due to an increase in the thermal energy entering the system, which enhances the efficiency of the absorption process. However, when a certain temperature is exceeded, the efficiency may decrease due to thermal losses and increased pressure within the system.

3.1.2 Effect of solution heat exchanger effectiveness (ε_1)

From Table 8, it is noted that the increased efficiency of heat exchangers leads to a marked improvement in COP, rising from 0.7906 at ε_1= 0.5 to 0.8482 at ε_1= 0.9. This is explained by improved energy recovery and a reduced amount of heat required from the generator (Q_g), which enhances the overall performance of the system

3.1.3 Effect of condenser temperature (T_c)

The COP decreased from 0.8402 at $\mathrm{T_c}$ = 25°C to 0.7906 at $\mathrm{T_c}$ = 40°C as the temperature of the condenser increased as shown in Table 8. This is due to the fact that an increase in $\mathrm{T_c}$ results in a rise in condensation pressure, which in turn negatively impacts the system's overall performance and reduces the efficacy of heat transfer.

3.1.4 Effect of absorber temperature (T_a)

Increasing the temperature of the absorbent shown in Table 8, a gradual decrease in the COP was observed. For example, the COP decreased from 0.8236 at T_a = 25°C to 0.7662 at T_a= 40°C. This is explained by the effect of absorbent temperature on the absorption process, as higher temperatures reduce the ability of the solution to absorb water vapor, reducing the efficiency of the process.

3.1.5 Effect of evaporator temperature (T_e)

As the evaporator heated, the COP increased from 0.7432 at T_e = 5°C to 0.8525 at T_e = 20°C. This indicates that higher temperatures in the evaporator improve the absorption efficiency and reduce the heat load required from the generator.

3.1.6 Effect of concentration of weak solution (Xws)

While investigating the impact of weak solution concentration, it was noted that an increase in Xws results in a decrease in COP shown in Table 8. Specifically, the coefficient of performance (COP) decreases from 0.8262 at Xws = 0.48 to 0.7648 at Xws = 0.54. This is a result of the reduction in cycle efficiency that results from the emphasis on vapor pressure and absorption efficiency.

Table 8
Performance parameter evaluation

Perimeters: $\boldsymbol{Q_a}$=5 KW, $\boldsymbol{T_a}$=35°C, $\boldsymbol{T_c}$=40 °C, $\boldsymbol{T_e}$=10 °C, $\boldsymbol{\varepsilon_1}$=0.5				
$\boldsymbol{Q_g}$	Q_a	Q_c	COP	T_g
6.549	6.458	5.119	0.7634	80
6.324	6.218	5.119	0.7906	90
6.279	6.167	5.119	0.7963	100
6.263	6.1422	5.119	0.7983	110
Perimeters: $\boldsymbol{Q_a}$=5 KW, $\boldsymbol{T_a}$=35°C, $\boldsymbol{T_c}$=40 °C, $\boldsymbol{T_e}$=10 °C, $\boldsymbol{T_g}$=90 °C				
$\boldsymbol{Q_g}$	Q_a	Q_c	COP	ε_1
6.324	6.218	5.119	0.7906	0.5
6.2171	6.109	5.119	0.8042	0.6
6.109	6.001	5.119	0.8184	0.7
6.002	5.893	5.119	0.8330	0.8
5.894	5.784	5.119	0.8482	0.9
Perimeters: $\boldsymbol{Q_a}$=5 KW, $\boldsymbol{T_a}$=35°C, $\boldsymbol{T_e}$=10 °C, $\boldsymbol{T_g}$=90 °C, $\boldsymbol{\varepsilon_1}$=0.5				
$\boldsymbol{Q_g}$	Q_a	Q_c	COP	T_c
5.951	5.894	5.058	0.8402	25
6.052	5.980	5.078	0.8261	30
6.169	6.080	5.099	0.8105	35
6.324	6.218	5.119	0.7906	40
Perimeters: $\boldsymbol{Q_a}$=5 KW, $\boldsymbol{T_c}$=40 °C, $\boldsymbol{T_e}$=10 °C, $\boldsymbol{T_g}$=90 °C, $\boldsymbol{\varepsilon_1}$=0.5				
$\boldsymbol{Q_g}$	Q_a	Q_c	COP	T_a

6.071	5.948	5.119	0.8236	25
6.182	6.067	5.119	0.8087	30
6.324	6.218	5.119	0.7906	35
6.526	6.432	5.119	0.7662	40
Perimeters: $\boldsymbol{Q_a}$=5 KW, $\boldsymbol{T_a}$=35°C, $\boldsymbol{T_c}$=40 °C, $\boldsymbol{T_g}$=90 °C, $\boldsymbol{\varepsilon_1}$=0.5				
$\boldsymbol{Q_g}$	Q_a	Q_c	COP	T_e
6.727	6.615	5.140	0.7432	5
6.324	6.218	5.119	0.7906	10
6.062	5.967	5.099	0.8247	15
5.864	5.785	5.079	0.8525	20
Perimeters: $\boldsymbol{Q_a}$=5 KW, $\boldsymbol{T_a}$=35°C, $\boldsymbol{T_c}$=40 °C, $\boldsymbol{T_e}$=10 °C, $\boldsymbol{T_g}$=90 °C, $\boldsymbol{\varepsilon_1}$=0.5				
$\boldsymbol{Q_g}$	Q_a	Q_c	COP	Xws
6.052	5.935	5.119	0.8262	0.48
6.178	6.066	5.119	0.8093	0.5
6.333	6.227	5.119	0.7894	0.52
6.537	6.439	5.119	0.7648	0.54

3.2 Implementation Challenges

Implementing a lithium-water bromide solution-based absorption cooling system in cars presents a difficult engineering task that mainly depends on using exhaust heat. System component integration for the generator, condenser, evaporator and absorbent becomes complicated because these elements must function within the vehicle's space constraints. The weight of major system elements coupled with spatial requirements creates barriers to car manufacturers whose priority is weight and space tier reduction. The production cost of this system exceeds traditional refrigeration systems since it needs lithium bromide solutions and special heat exchangers and pumps, among other high-efficiency components. Additionally, the development expenses for this system tend to be higher than conventional refrigeration systems. Having to follow EPA and EU regulations for vehicle cooling systems creates another obstacle for compliance since both bodies demand specific standards related to thermal efficiency and operational safety for vehicles. The dynamic performance of the system may also be affected by exhaust temperature changes while driving, which requires the development of advanced control systems to improve its response to these changes and ensure the stability of its performance. Despite these challenges, environmental benefits and reduced energy consumption make absorption cooling a promising option for vehicle air conditioning systems, provided that compact and lightweight designs are developed, heat exchanger efficiency is improved and intelligent control technologies are enhanced to ensure optimal operation of the system under different operating conditions.

4. Conclusion

This study investigates a 5-kW ACS that employs a water-lithium bromide solution as its working fluid. The apparatus is connected to engine exhaust gas, which produces waste heat at varying temperatures. The thermodynamic model, which was developed in accordance with the “first law of thermodynamics”, was employed to analyse the system's performance theoretically. This model was applied to each component of the system. The binary mixture thermodynamic properties are accurately calculated by coupling the model to a set of states of equations. To facilitate a thermodynamic analysis of the system under a range of operating conditions, the temperatures of the generator, condenser, absorber and evaporator have been adjusted, respectively. Even at low temperatures, the condenser and absorber of the cycle operate at their optimum performance.

The results showed that increasing the temperature of the generator and evaporator leads to an increase in the absorption refrigeration system performance coefficient. The performance coefficient was 0.8228 at the temperatures of the evaporator, generator, condenser and absorbent (15, 90, 40 and 35 °C, respectively). In the same condition, the cop was 0.7398 at 5°C evaporator temperature. The results also showed that the performance coefficient of the absorption refrigeration system decreases as the temperature of the generator, absorber and condenser increases. The COP was 0.7617 at 40°C for the condenser and 90 °C for the generator. Under identical conditions, the COP was 0.8082 at a condenser temperature of 30°C. The COP increases as a consequence of the solution heat exchanger's increased effectiveness, the COP was 0.7781 at the condenser, evaporator, generator and absorber and effectiveness (40, 7, 90, 35 °C and 0.6), at the same condition of temperature and 0.9 effectiveness heat exchanger the COP was 0.8321, while the circulation ratio remains unaffected. The results also indicated that increasing the X_{ws} negatively affects the COP by reducing the absorber heat absorption capacity, increasing energy consumption and raising pressure, while a higher X_{ss} from the generator improves thermal efficiency and system stability at lower absorber temperatures

Acknowledgement

I would like to express my gratitude to the University of Basra, College of Engineering, Department of Mechanical Engineering for their support and for providing the opportunity to conduct this research. I also extend my special thanks to my supervisor, Professor Dr. Salman Hashim Hamadi, for his valuable guidance and continuous support.

References

[1] Fu, Jianqin, Jingping Liu, Renhua Feng, Yanping Yang, Linjun Wang and Yong Wang. "Energy and exergy analysis on gasoline engine based on mapping characteristics experiment." *Applied energy* 102 (2013): 622-630. https://doi.org/10.1016/j.apenergy.2012.08.013

[2] Khudhur, Jawad, Abdulrazzak Akroot and Ahmed Al-Samari. "Experimental Investigation of Direct Solar Photovoltaics that Drives Absorption Refrigeration System." *Journal Of Advanced Research In Fluid Mechanics And Thermal Sciences* 1, no. 1 (2023): 116-135. https://doi.org/10.37934/arfmts.106.1.116135

[3] Taylor, Alex MKP. "Science review of internal combustion engines." *Energy policy* 36, no. 12 (2008): 4657-4667. https://doi.org/10.1016/j.enpol.2008.09.001

[4] Zhang, L. Z. "Design and testing of an automobile waste heat adsorption cooling system." *Applied thermal engineering* 20, no. 1 (2000): 103-114. https://doi.org/10.1016/S1359-4311(99)00009-5

[5] Shu, Gequn, Youcai Liang, Haiqiao Wei, Hua Tian, Jian Zhao and Lina Liu. "A review of waste heat recovery on two-stroke IC engine aboard ships." *Renewable and Sustainable Energy Reviews* 19 (2013): 385-401. https://doi.org/10.1016/j.rser.2012.11.034

[6] AlQdah, Khaled S. "Performance and evaluation of aqua ammonia auto air conditioner system using exhaust waste energy." *Energy procedia* 6 (2011): 467-476. https://doi.org/10.1016/j.egypro.2011.05.054

[7] Karamangil, M. I., S. Coskun, O. Kaynakli and N. Yamankaradeniz. "A simulation study of performance evaluation of single-stage absorption refrigeration system using conventional working fluids and alternatives." *Renewable and Sustainable Energy Reviews* 14, no. 7 (2010): 1969-1978. https://doi.org/10.1016/j.rser.2010.04.008

[8] Starace, Giuseppe and Lorenzo De Pascalis. "An enhanced model for the design of diffusion absorption refrigerators." *International Journal of Refrigeration* 36, no. 5 (2013): 1495-1503. https://doi.org/10.1016/j.ijrefrig.2013.02.016

[9] Zohar, A., M. Jelinek, A. Levy and I. Borde. "Numerical investigation of a diffusion absorption refrigeration cycle." *International Journal of Refrigeration* 28, no. 4 (2005): 515-525. https://doi.org/10.1016/j.ijrefrig.2004.11.003

[10] Chua, H. T., H. K. Toh and Kim Choon Ng. "Thermodynamic modeling of an ammonia–water absorption chiller." *International Journal of Refrigeration* 25, no. 7 (2002): 896-906. https://doi.org/10.1016/S0140-7007(01)00101-3

[11] Misra, R. D., Pradeep K. Sahoo and A. Gupta. "Thermoeconomic evaluation and optimization of an aqua-ammonia vapour-absorption refrigeration system." *International Journal of Refrigeration* 29, no. 1 (2006): 47-59. https://doi.org/10.1016/j.ijrefrig.2005.05.015

[12] Koehler, J., W. J. Tegethoff, D. Westphalen and M. Sonnekalb. "Absorption refrigeration system for mobile applications utilizing exhaust gases." *Heat and Mass Transfer* 32, no. 5 (1997): 333-340. https://doi.org/10.1007/s002310050130

[13] Lin, L., Y. Wang, T. Al-Shemmeri, S. Zeng, J. Huang, Y. He, X. Huang, S. Li and J. Yang. "Characteristics of a diffusion absorption refrigerator driven by the waste heat from engine exhaust." *Proceedings of the Institution of Mechanical Engineers, Part E: Journal of Process Mechanical Engineering* 220, no. 3 (2006): 139-149. https://doi.org/10.1243/09544089JPME102

[14] Manzela andré Aleixo, Sérgio Morais Hanriot, Luben Cabezas-Gómez and José Ricardo Sodré. "Using engine exhaust gas as energy source for an absorption refrigeration system." *Applied energy* 87, no. 4 (2010): 1141-1148. https://doi.org/10.1016/j.apenergy.2009.07.018

[15] Anurodh Mohapatra, Karan Kumar Aneja R, Sagar Kadam, Aaqib Rafiq, Alekh Anil. " Heat Recovery System in Automobile." *International Journal of Scientific Research in Computer Science, Engineering and Information Technology (IJSRCSEIT),* Volume 4, Issue 5, (2018): 268-271.

[16] Rêgo, A. T., S. M. Hanriot, A. F. Oliveira, P. Brito and T. F. U. Rêgo. "Automotive exhaust gas flow control for an ammonia–water absorption refrigeration system." *Applied thermal engineering* 64, no. 1-2 (2014): 101-107. https://doi.org/10.1016/j.applthermaleng.2013.12.018

[17] Hilali, Ismail and Mehmet Sait SÖYLEMEZ. "An Application Of Engine Exhaust Gas Driven Cooling System In Automobile Air-Conditioning System." *Journal of Thermal Science & Technology/Isı Bilimi ve Tekniği Dergisi* 35, no. 1 (2015).

[18] Aly, Wael IA, Mohammed Abdo, Gamal Bedair and A. E. Hassaneen. "Thermal performance of a diffusion absorption refrigeration system driven by waste heat from diesel engine exhaust gases." *Applied Thermal Engineering* 114 (2017): 621-630. https://doi.org/10.1016/j.applthermaleng.2016.12.019

[19] Adjibade, Mohamed Izzedine Serge, Ababacar Thiam, Christophe Awanto and Dorothé Azilinon. "Experimental analysis of diffusion absorption refrigerator driven by electrical heater and engine exhaust gas." *Case studies in thermal engineering* 10 (2017): 255-261. https://doi.org/10.1016/j.csite.2017.07.004

[20] Yuan, Han, Ji Zhang, Xiankun Huang and Ning Mei. "Experimental investigation on binary ammonia–water and ternary ammonia–water–lithium bromide mixture-based absorption refrigeration systems for fishing ships." *Energy Conversion and Management* 166 (2018): 13-22. https://doi.org/10.1016/j.enconman.2018.04.013

[21] Kaewpradub, Sorawit, Prawit Sanguanduean, Wattanapong Katesuwan, Nares Chimres, Phatthi Punyasukhananda, Lazarus Godson Asirvatham, Omid Mahian, Ahmet Selim Dalkilic and Somchai Wongwises. "Absorption refrigeration system using engine exhaust gas as an energy source." *Case studies in thermal engineering* 12 (2018): 797-804. https://doi.org/10.1016/j.csite.2018.10.003

[22] Kaynakli, Omer and Muhsin Kilic. "Theoretical study on the effect of operating conditions on performance of absorption refrigeration system." *Energy conversion and management* 48, no. 2 (2007): 599-607. https://doi.org/10.1016/j.enconman.2006.06.005

[23] Sharma, Anil, Bimal Kumar Mishra, Abhinav Dinesh and Ashok Misra. "Design and performance study of a hot water driven 5 TR capacity absorption cooling system." *Int. J. U-E-Serv. Sci. Technol* 7 (2014): 205-212. https://doi.org/10.14257/ijunesst.2014.7.6.18

[24] Palomba, Valeria, Marcello Aprile, Mario Motta and Salvatore Vasta. "Study of sorption systems for application on low-emission fishing vessels." *Energy* 134 (2017): 554-565. https://doi.org/10.1016/j.energy.2017.06.079

[25] Zheng, Jian, J. Castro, A. Oliva and C. Oliet. "Energy and exergy analysis of an absorption system with working pairs LiBr-H2O and Carrol-H2O at applications of cooling and heating." *International Journal of Refrigeration* 132 (2021): 156-171. https://doi.org/10.1016/j.ijrefrig.2021.09.011

[26] Kumar, J. Jayadeep and James Varghese. "Modeling, optimizing and sizing of a solar air conditioning system with refrigerant storage for meeting the 24-hour cooling load of a restaurant building." *International Journal of Thermofluids* 20 (2023): 100472. https://doi.org/10.1016/j.ijft.2023.100472

[27] Ammar, Nader R. and Ibrahim S. Seddiek. "Thermodynamic, environmental and economic analysis of absorption air conditioning unit for emissions reduction onboard passenger ships." *Transportation Research Part D: Transport and Environment* 62 (2018): 726-738. https://doi.org/10.1016/j.trd.2018.05.003

[28] Tawalbeh, Muhammad, Tareq Salameh, Mona Albawab, Amani Al-Othman, Mamdouh El Haj Assad and Abdul H. Alami. "Parametric study of a single effect lithium bromide-water absorption chiller powered by a renewable heat source." *Journal of Sustainable Development of Energy, Water and Environment Systems* 8, no. 3 (2020): 464-475. https://doi.org/10.13044/j.sdewes.d7.0290

[29] Ebrahimi, Khosrow, Gerard F. Jones and Amy S. Fleischer. "Thermo-economic analysis of steady state waste heat recovery in data centers using absorption refrigeration." *Applied Energy* 139 (2015): 384-397. https://doi.org/10.1016/j.apenergy.2014.10.067

[30] Kaita, Y. "Thermodynamic properties of lithium bromide–water solutions at high temperatures." *International Journal of refrigeration* 24, no. 5 (2001): 374-390. https://doi.org/10.1016/S0140-7007(00)00039-6

[31] Babu, B. and G. Maruthi Prasad Yadav. "Performance analysis of lithium-bromide water absorption refrigeration system using waste heat of boiler flue gases." *International Journal of Engineering Research and Management (IJMERM) ISSN* (2015): 2349-2058.

[32] Rubio-Maya, Carlos, J. Jesús Pacheco-Ibarra, Juan M. Belman-Flores, Sergio R. Galván-González and Crisanto Mendoza-Covarrubias. "NLP model of a LiBr–H2O absorption refrigeration system for the minimization of the annual operating cost." *Applied Thermal Engineering* 37 (2012): 10-18. https://doi.org/10.1016/j.applthermaleng.2011.12.035

[33] Patel, Haresh A., L. N. Patel, Darshan Jani and Amit Christian. "Energetic analysis of single stage lithium bromide water absorption refrigeration system." *Procedia Technology* 23 (2016): 488-495. https://doi.org/10.1016/j.protcy.2016.03.054